

International Journal of Modern Physics D  
 © World Scientific Publishing Company

## HIGH-ENERGY PARTICLE INTERACTIONS IN THE INNER JET OF THE RADIO GALAXY M87

Chloé Guennou

*Université Paris XI, Orsay Campus  
 Orsay, 91400, France  
 chloe.guennou@u-psud.fr*

Gustavo E. Romero

Gabriela S. Vila

*Instituto Argentino de Radioastronomía  
 C.C.5, Villa Elisa, 1894, Buenos Aires, Argentina  
 romero@iar.unlp.edu.ar - gvila@iar.unlp.edu.ar*

Received 23 December 2009

Revised 4 February 2010

Communicated by Managing Editor

Recent observations with the High Energy Stereoscopic System (HESS) have revealed strong and variable high-energy gamma-ray emission from the radio galaxy M87. The origin of such emission is uncertain, but the rapid variability indicates that it should be produced close to the central engine of the source. In this work, a lepto-hadronic one-zone model is applied to the available multiwavelength data of M87. The different energy losses for both primary and secondary particles are calculated. Then, the different contributions to the spectral energy distribution through interactions with matter, radiation and magnetic fields are obtained, in good accordance with the observations.

*Keywords:* Radiation mechanisms: non-thermal, galaxies: jets, galaxies: individual: M87

### 1. Introduction

The radio galaxy M87 is one of the closest radio galaxies and one of the first to be recognized as a powerful source of radio emission. Located at  $\sim 16$  Mpc ( $z=0.0043$ ) in the Virgo cluster, M87 harbours a black hole of  $\sim 3 \times 10^9 M_{\odot}$ .<sup>1</sup> It still arouses great interest today because it has been suggested to be an accelerator of Ultra-High-Energy Cosmic Rays,<sup>2</sup> and because of the detection of fast variations in its TeV gamma-ray flux. The jet in M87 is oriented at an angle of  $15^{\circ}$  with respect to the observer's line of sight<sup>3</sup> and it is the best-resolved jet on subparsec scales. The length scale of the jet is about 2 kpc.<sup>4</sup> Superluminal motion with apparent velocity of about  $4-6c$  has been observed between 1994 and 1998 by the Hubble Space Telescope (HST),<sup>3</sup> confirming the relativistic nature of the outflow. M87 has been observed all along the electromagnetic spectrum with different instruments,

like the HST in optical wavelengths,<sup>3,5,6</sup> the Very Large Array (VLA) in the radio band,<sup>7</sup> and the *Chandra* satellite in X-rays.<sup>8,9</sup> The Cherenkov telescopes High Energy Stereoscopic System (HESS),<sup>10</sup> the Major Atmospheric Gamma-ray Imaging Cherenkov Telescope (MAGIC)<sup>11</sup> and the Very Energetic Radiation Imaging Telescope Array System (VERITAS)<sup>12</sup> have also observed M87 in gamma rays, including a jointly coordinated campaign in 2008.<sup>13</sup> The correlation between the emission in radio, optical and X-rays suggests a common radiation mechanism at all wavelengths.<sup>14</sup>

Recently, observations carried out with HESS showed fast variability with a timescale of two days in the range of  $\gamma$ -rays, ten times faster than in other wavebands. These observations imply a very compact acceleration region with a size of the order of ten gravitational radius,  $10R_g \sim 4.5 \times 10^{15}$  cm (for further details see Ref. 15).

In this work we present a jet model set up to fit the observed spectrum of M87, from radio to gamma rays. The model is based on that developed in Ref. 16; we describe it briefly in Sect. 2. In Sect. 3, we present the application to M87 and the best-fit spectral energy distribution (SED) obtained. Finally, in Sect. 4 we close with a discussion of the results and the perspectives for future works.

## 2. Model

### 2.1. Jet model

We assume that the point of kinetic launching of the jet (where Poynting flux is converted to kinetic energy flux) is located at a distance  $z_0 = 50R_g$  from the black hole. The outflow then expands as a cone with a half-opening angle  $\phi$ . In the one-zone approximation,<sup>17</sup> the acceleration of particles up to relativistic energies takes place in a compact region. The distance from the black hole to the one-zone is  $z_{\text{acc}}$ . The acceleration region extends up to a certain  $z_{\text{max}}$  and has a thickness  $\Delta z = z_{\text{max}} - z_{\text{acc}} = R_{\text{jet}}(z_{\text{acc}})/4$ , where  $R_{\text{jet}}(z)$  is the jet radius. We assume that particles gain energy through diffusive shock acceleration.

If the jet expands adiabatically, the magnetic field decreases with the distance to the black hole,

$$B(z) = B_0 \left( \frac{z}{z_0} \right)^{-m}, \quad (1)$$

with  $1 < m < 2$ . The value of  $B_0 = B(z_0)$  is calculated assuming equipartition between the kinetic and magnetic energy densities at  $z_0$ .<sup>18</sup> The value of  $z_{\text{acc}}$  is determined demanding sub-equipartition between the magnetic and matter energy densities.

The estimated value of the jet kinetic luminosity in M87 is  $L_{\text{jet}} \approx 10^{44}$  erg s<sup>-1</sup>.<sup>5</sup> We assume that a fraction of this power is in the form of relativistic particles:  $L_{\text{rel}} = q_{\text{rel}} L_{\text{jet}}$  with  $L_{\text{rel}} = L_p + L_e$ . Here  $L_p$  and  $L_e$  are the luminosities in relativistic

hadrons and leptons, respectively. The ratio  $a = L_p/L_e$  is unknown, and we leave it as a free parameter.

## 2.2. Relativistic particle distributions

We assume an injection spectrum of relativistic electrons and protons that is a power law,

$$Q_{e,p}(E_{e,p}) = Q_{0_{e,p}} E^{-\alpha} \quad [Q] = \text{erg}^{-1} \text{s}^{-1} \text{cm}^{-3}. \quad (2)$$

The value of the constant  $Q_{0_{e,p}}$  can be obtained from the total luminosity injected in each type of particle (see Ref. 16 for details of the calculations).

We take into account several radiative cooling processes for protons and electrons, as well as adiabatic losses since the jet expands laterally. The maximum energy for each type of particle is obtained by balance of the sum of the cooling rates and the acceleration rate, given by

$$t_{\text{acc}}^{-1} = \frac{\eta e c B}{E} \quad (3)$$

with  $\eta < 1$  a free parameter that determines the acceleration efficiency. As it can be seen from Figure 1, the most relevant cooling processes for both protons and electrons are synchrotron radiation and adiabatic losses, and also  $pp$  interactions in the case of protons.

To calculate the proton and electron energy distributions  $N(E)$ , we solve the steady-state transport equation in the one-zone approximation.<sup>17</sup> As well as energy losses and particle injection, we include in this equation a particle escape term  $N(E)/t_{\text{esc}}$ .<sup>16</sup> The resulting distributions have a power-law dependence on the particle energy:  $N(E) \propto E^{-\alpha}$ .

## 2.3. Radiative processes

In our model the most relevant radiative process are synchrotron radiation, inverse Compton scattering (IC), proton-proton ( $pp$ ) and proton-photon ( $p\gamma$ ) inelastic collisions, and Bremsstrahlung radiation. We calculate the electromagnetic emission from each mechanism using standard formulas, see Ref. 16 for details.

We also calculate the radiative contribution of secondary pions, muons and electron-positron pairs created in  $pp$  and  $p\gamma$  interactions. The steady-state energy distributions of these particles are obtained as for primary electrons and protons including, in the case of pions and muons, the decay time in the escape term. For further details see Ref. 16 and references therein.

### 3. Application to M87

The values of the model parameters are compiled in Table 1; only  $a$ ,  $z_{\text{acc}}$  and  $E_{\text{min}}$  (the same for protons and primary electrons) were varied during the fitting. For a jet kinetic power  $L_{\text{jet}} \approx 10^{44} \text{ erg s}^{-1}$ , the magnetic field at the jet base is  $B_0 \approx 84 \text{ G}$ ; it then decays as  $B \propto z^{-m}$  with  $m = 2$ . The power injected in relativistic particles is a fraction  $q_{\text{jet}} = 0.1$  of  $L_{\text{jet}}$ . We consider a proton-dominated jet with a hadron-to-lepton power ratio  $L_p/L_e = a = 50$ . We fix  $\eta = 0.1$  (efficient acceleration) and a canonical particle injection spectral index  $\alpha = 2.2$ .

Table 1. Parameters used to generate SED.

Parameter	[units]	Value
$M_*$	Black hole mass [ $M_\odot$ ]	$3 \times 10^9$
$L_{\text{jet}}$	Jet power [ $\text{erg s}^{-1}$ ]	$10^{44}$
$\Gamma_{\text{jet}}$	Jet bulk Lorentz factor	4.5
$\theta$	Jet viewing angle	$15^\circ$
$\phi$	Jet half-opening angle	$5^\circ$
$z_0$	Jet launching point [ $R_g$ ]	50
$B_0$	Magnetic field at the base of the jet [G]	$\sim 84$
$m$	Magnetic field decay index	2
$q_{\text{jet}}$	Jet content of relativistic particles	0.1
$a$	Hadron-to-lepton power ratio	50
$\eta$	Acceleration efficiency	0.1
$\alpha$	Particle injection spectral index	2.2
$E_{\text{min}}$	Minimum particle energy [ $mc^2$ ]	100
$z_{\text{acc}}$	Distance BH-acceleration region	$\sim 45 z_0$

The values of jet luminosity and the viewing angle are taken from Ref. 5.

Figure 1 shows the acceleration and cooling rates for protons and electrons; also shown is the escape rate, that we approximate as  $t_{\text{esc}}^{-1} \approx v_{\text{jet}}/\Delta z$ . The maximum energies for protons and electrons are  $E_p^{\text{max}} \approx 3 \times 10^{18} \text{ eV}$  and  $E_e^{\text{max}} \approx 1.5 \times 10^{14} \text{ eV}$ , respectively. For the electrons the main cooling process is synchrotron radiation, whereas adiabatic losses are the most relevant channel for the protons.

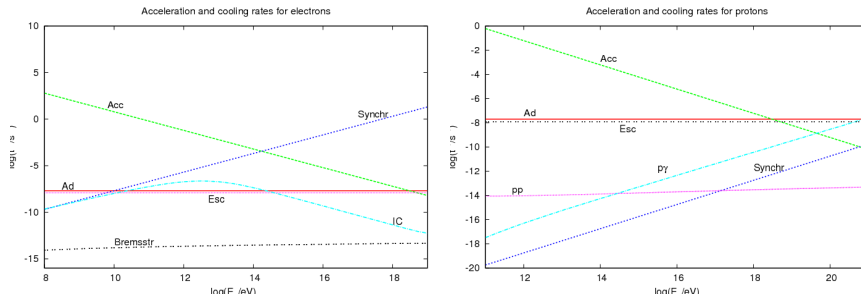


Fig. 1. Acceleration, escape and cooling rates for electrons (left) and protons (right) in the one-zone.

Figure 2 shows the best-fit SED obtained for the parameters in Table 1. The three main contributions to the luminosity are electron synchrotron radiation and IC scattering peaking at  $\sim 10^{40}$  erg s $^{-1}$ , and  $p\gamma$  interaction peaking at  $\sim 10^{39}$  erg s $^{-1}$ . All radiation emitted by secondary particles is negligible: synchrotron radiation of secondary electron-positron pairs peaks at  $\sim 10^{37}$  erg s $^{-1}$  and IC scattering at  $\sim 10^{35}$  erg s $^{-1}$ . The fit to the radio, optical-UV and gamma-ray data is good, but the X-ray emission is overpredicted by the model. However, as X-rays may be absorbed in the interstellar medium of the galaxy, the intrinsic flux from the source may be higher than the observed flux. We did not perform any corrections to the data to obtain the “deabsorbed” flux.

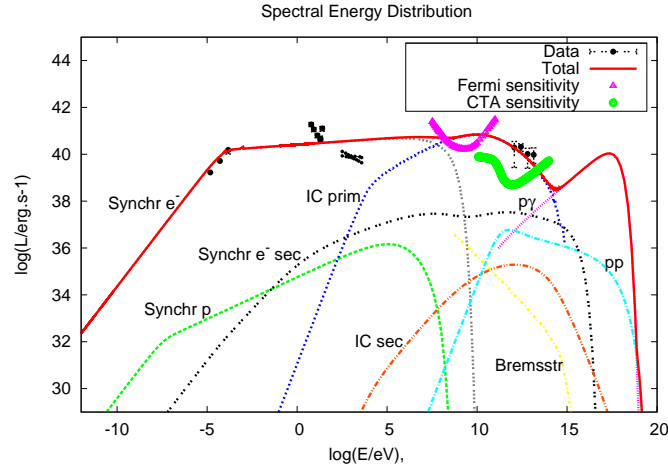


Fig. 2. Spectral energy distribution obtained for the values of the parameters showed in Table 1. The sensitivities of the Cherenkov Telescope Array (CTA) and the Fermi gamma-ray telescope are also shown. The data are not simultaneous. See Ref. 19 and references therein for a discussion on the observations.

We have also calculated the opacity  $\tau_{\gamma\gamma}$  for photon absorption due to  $\gamma\gamma$  annihilation in the internal jet radiation field. This process is important in some models and TeV emission can be absorbed. However, for the model of Figure 2 the spectral energy distribution is not affected. The radiation is completely suppressed only above  $\sim 10^8$  TeV, what is of no observable consequence.

#### 4. Discussion and perspectives

The model presented here explains the observed broadband emission from M87 mainly with leptonic contributions. The hadronic contribution becomes dominant only at very high energies, between  $\sim 10^{14}$  and  $\sim 10^{19}$  eV. For such energies M87 may be an important source of neutrinos injected through pion and muon decay. The number of muon neutrinos that might be observed should be similar to the

number of photons. The future European neutrino detector KM3NET, expected to operate around 2015, might detect this emission.

Further steps in our modeling of the M87 SED will consist in the introduction of a mechanism capable of explaining the observed variability, and the effect of convection in the transport of particles in the inner jet.

### Acknowledgments

We are grateful to CONICET, IAR and the University of Paris XI for supporting this work. C.G. specially thanks the GARRA group. This research was supported by ANPCyT through grant PICT-2007-00848 BID 1728/OC-AR.

### References

1. F. Macchetto et al., *ApJ* **489** (1997) 579.
2. R.J. Protheroe et al., *Astropart. Phys.* **19** (2003) 559.
3. J.A. Biretta, W.B. Sparks and F. Macchetto, *ApJ* **520** (1999) 621.
4. H.L. Marshall et al., *ApJ* **564** (2002) 683.
5. C.-C. Wang and H.-Y. Zhou, *Mon. Not. R. Astron. Soc.* **1** (2009) 11.
6. J.P. Madrid, *Astron. J.* **4** (2009) 3864.
7. F.N. Owen, P.E. Hardree, and T.J. Cornwell, *ApJ* **340** (1989) 698.
8. A.S. Wilson and Y. Yang, *ApJ* **568** (2002) 133.
9. D.E. Harris, C.C. Cheung, J.A. Biretta, W.B. Sparks, E.S. Perlman and A.S. Wilson, *ApJ* **640** (2006) 221.
10. W. Hofmann, H.E.S.S. highlights, in *Proc., 29th Int. Cosmic Ray Conf.*, eds. B. Sripathi Acharya, S. Gupta, P. Jagadeesan, A. Jain, S. Karthikeyan, S. Morris and S. Tonwar (Pune, 2005), p. 97.
11. MAGIC Collab. (J. Albert et al.), *ApJ* **685** (2008) L23.
12. VERITAS Collab. (V.A. Acciari et al.), *ApJ* **679** (2008) 397.
13. V.A. Acciari et al., *Science* **325** (2009) 444.
14. E.S. Perlman, J.A. Biretta, W.B. Sparks, F.D. Macchetto and J.P. Leahy, *ApJ* **551** (2001) 206.
15. F.A. Aharonian et al., *Science* **314** (2006) 1424.
16. G.E. Romero and G.S. Vila, *A&A* **3** (2008) 485.
17. D. Khangulyan, S. Hnatic, F.A. Aharonian and S. Bogovalov, *Mon. Not. R. Astron. Soc.* **380** (2007) 320.
18. V. Bosch-Ramon, G.E. Romero and J.M. Paredes, *A&A* **447** (2006) 263.
19. J.P. Lenain, C. Boisson, H. Sol and K. Katarzynski, *ApJ* **111** (2008) 120.